Environmental Science & Technology

Article

pubs.acs.org/est

# Isotopic Composition of Gaseous Elemental Mercury in the Free Troposphere of the Pic du Midi Observatory, France

Xuewu Fu,*[,†,‡] Nicolas Marusczak,[†] Xun Wang,[‡] François Gheusi,[§] and Jeroen E. Sonke*[,†]

[†]Observatoire Midi-Pyrénées, Laboratoire Géosciences Environnement Toulouse, CNRS/IRD/Université de Toulouse, 14, avenue Édouard Belin, 31400 Toulouse, France

[‡]State Key Laboratory of Environmental Geochemistry, Institute of Geochemistry, Chinese Academy of Sciences, 46 Guanshui Road 550002, Guiyang, China

[§]Observatoire Midi-Pyrénées, Laboratoire d'Aérologie, CNRS/IRD/Université de Toulouse, 14, avenue Édouard Belin, 31400 Toulouse, France

Supporting Information

**ABSTRACT:** Understanding the sources and transformations of mercury (Hg) in the free troposphere is a critical aspect of global Hg research. Here we present one year of observations of atmospheric Hg speciation and gaseous elemental Hg (GEM) isotopic composition at the high-altitude Pic du Midi Observatory (2860 m above sea level) in France. Biweekly integrated GEM from February 2012 to January 2013 revealed significant variations in $\delta^{202}Hg_{GEM}$ (−0.04‰ to 0.52‰) but not in $\Delta^{199}Hg_{GEM}$ (−0.17‰ to −0.27‰) or $\Delta^{200}Hg_{GEM}$ (−0.10‰ to 0.05‰). $\delta^{202}Hg_{GEM}$ was negatively correlated with CO and reflected air mass origins from Europe (high CO, low $\delta^{202}Hg_{GEM}$) and from the Atlantic Ocean (low CO, high $\delta^{202}Hg_{GEM}$). We suggest that the $\delta^{202}Hg_{GEM}$ variations represent mixing of recent low $\delta^{202}Hg_{GEM}$ European anthropogenic emissions with high $\delta^{202}Hg_{GEM}$ northern hemispheric background GEM. In addition, Atlantic Ocean free troposphere air masses showed a positive correlation between $\delta^{202}Hg_{GEM}$ and gaseous oxidized Hg (GOM) concentrations, indicative of mass-dependent Hg isotope fractionation during GEM oxidation. On the basis of atmospheric $\delta^{202}Hg_{GEM}$ and speciated Hg observations, we suggest that the oceanic free troposphere is a reservoir within which GEM is readily oxidized to GOM.

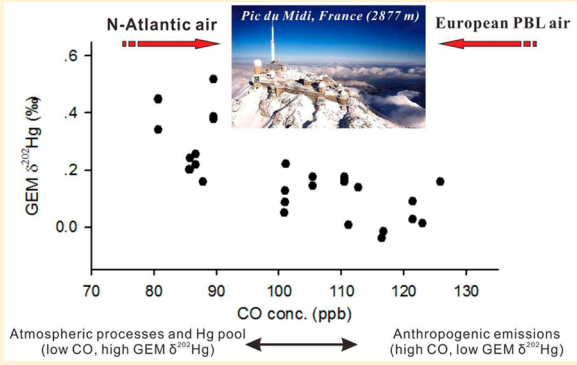


## INTRODUCTION

Mercury (Hg), especially in its methylated form, is a toxic pollutant to humans and wildlife. Both anthropogenic and natural sources emit Hg to the atmosphere. Hg released from anthropogenic sources mainly comes from the mining, energy, and metal refining sectors.[1,2] The fate of anthropogenic Hg emissions is determined by the reactivity of the various atmospheric forms of Hg. Atmospheric Hg can be operationally separated into three major forms: gaseous elemental mercury (GEM), gaseous oxidized mercury (GOM), and particulate bound mercury (PBM), with the sum of GEM and GOM known as total gaseous mercury (TGM). GEM, the dominant form of total Hg in the lower atmosphere (>75%), is fairly stable with a residence time of several months to a year and is therefore globally dispersed by atmospheric circulation.[3,4] GOM and PBM have shorter residence times, on the order of days to weeks, due to rapid scavenging followed by deposition.[5] Linking Hg deposition to Hg emission sources is one of the main knowledge gaps in Hg science, and substantial interest exists in the development of appropriate tracers.[6]

During the past decade, significant advances have been made in the measurement of Hg isotopic compositions of geogenic and biological materials.[7] Laboratory evidence suggests that processes controlling Hg emission such as reduction−oxidation, adsorption−desorption, or volatilization can induce significant mass-dependent Hg isotope fractionation (MDF, $\delta^{202}Hg$ signature).[8−12] Unusual mass-independent fractionation (MIF) of odd Hg isotopes has been observed for photochemical Hg reduction in water and snow ($\Delta^{199}Hg$, $\Delta^{201}Hg$ signatures).[8,13,14] Finally, Hg in wet deposition has been shown to carry even Hg isotope MIF signatures ($\Delta^{200}Hg$, $\Delta^{204}Hg$)[12,15,16] that have been speculated to originate in GEM photo-oxidation above the tropopause.[16] The exact even-MIF mechanism remains unknown however. The MDF and MIF signatures of atmospheric GEM, GOM, and PBM therefore carry information on the transformations these species have undergone and on their potential emission sources.

Several studies have carried out measurements of TGM isotopic composition.[12,14,15,17] These studies were carried out at low altitude sites and therefore reflect mostly local sources and

Received: January 4, 2016
Revised: May 16, 2016
Accepted: May 23, 2016
Published: May 23, 2016





DOI: 10.1021/acs.est.6b00033
Environ. Sci. Technol. 2016, 50, 5641−5650

boundary layer processes. An early study in the Great Lakes region of the United States found $\delta^{202}Hg_{TGM}$ at industrial impacted sites to be lower than at rural sites.[15] A more recent study combined Hg isotope, meteorology, and back-trajectory modeling to characterize different Hg sources in coastal Pensacola, FL (United States).[18] The authors suggest the background global atmospheric mercury pool to be characterized by positive $\delta^{202}Hg_{TGM}$ values and also observed urban−industrial emissions to drive $\delta^{202}Hg_{TGM}$ to more negative values.

In the present study, we conducted one year of biweekly integrated measurements of atmospheric TGM isotopic composition along with atmospheric Hg speciation at the high-altitude Pic du Midi Observatory (PDM; 2860 m above sea level, France). PDM regularly receives air masses that are representative of the free troposphere and is situated close to the North Atlantic Ocean (minimum distance = 150 km). The data set we acquired presents a unique opportunity for studying the isotopic signatures of air masses originating from the European boundary layer and Atlantic Ocean free troposphere. The free troposphere (and stratosphere) is an important reservoir for depletion of GEM and production of GOM.[19−23] The relationships between isotopic compositions and transformation of atmospheric Hg may therefore also provide clues to better understand atmospheric Hg isotope chemistry and Hg redox chemistry.

## MATERIALS AND METHODS

**Site Description.** The Pic du Midi Observatory (PDM, 0.167° E, 43.067° N, 2860 m above sea level, http://geomon.empa.ch/index.php?id=PDM) is a high-altitude monitoring station situated on top of an isolated peak on the north edge of the central Pyrenees Mountains, Southwest France. The Pyrenees stretch ∼491 km from the North Atlantic Ocean to the Mediterranean Sea with a maximum width of approximately 110 km in the central area. The PDM Observatory receives free tropospheric air from the East Atlantic Ocean and Europe and boundary layer air mostly from southwest France. At the synoptic scale, the station is under the dominant influence of winds in the northwestern quadrant, but advection from Spain and North Africa (mostly in spring and autumn) or from northwestern Europe (mostly in winter) are not rare.[24] There are no Hg emission point sources around the station or in the surrounding areas. The two nearest cities are Pau and Tarbes, which are located 60 and 30 km northwest to the station, respectively, and are thought to have a limited impact on the station owing to rare northwesterly upslope winds.

**Atmospheric TGM Collection and Processing.** TGM in ambient air at PDM was collected on iodine- (IC) and chlorine-impregnated activated carbon (CLC) traps. Iodine-impregnated activated carbon was purchased from Brooks Rand Inc. (Seattle, WA, United States) and chlorine-impregnated activated carbon was prepared in the lab using 0.15 N double-distilled HCl. Detailed information regarding the preparation of chlorine-impregnated activated carbon can be found in Fu et al.[25] Sampling of TGM isotopes was conducted from February 13, 2012 to January 25, 2013 using 250 mg IC or CLC traps and collected atmospheric TGM for a sampling duration of 15−20 days (biweekly samples) at a flow rate of 1.3−2.4 LPM. IC and CLC traps collect atmospheric TGM efficiently (>95%) at the given sampling flow rates.[25] The sampling flow rate and duration of the two types of traps enabled sufficient collection of atmospheric TGM for isotopic analysis (>12 ng). Blanks of IC and CLC were determined using a DMA-80 automatic mercury analyzer and showed mean values <0.3 ng $g^{-1}$, which was negligible.

The sampling inlets of the IC and CLC traps were connected to a Tekran 1104 Teflon-coated, heated manifold, which pulled outside air into the lab. The manifold inlet protruded ∼0.5 m from the outside wall into the prevailing southwest wind direction at PDM. Ambient air was pulled through the manifold at a constant flow rate of ∼100 LPM using a blower unit. To remove air particles, precleaned quartz filters were installed at the inlets of IC and CLC traps. All the traps were kept warm (50−70 °C) during sampling using silicone rubber heating pads (RadioSpares) to prevent water condensation. Sampling flow rates of IC and CLC traps were controlled via gas flow meters installed at the outlets of the vacuum pumps, and the total sampling volumes of the traps were recorded using gas meters, calibrated with a Bios Defender (Mesalabs, United States).

After the completion of field sampling, IC and CLC traps were sealed with silicone stoppers and three successive polyethylene bags and stored in a clean environment until preconcentration into trap solutions for Hg isotope analysis. Detailed information regarding the preconcentration of Hg from IC and CLC traps into solutions can be found in Fu et al.[25] Briefly, Hg in CLC traps was thermally decomposed in a Hg-free oxygen flow (25 mL $min^{-1}$), and then the combustion products were carried off and further decomposed in a hot quartz tube (1000 °C). The combustion released all the Hg in the form of $Hg^0$, which was subsequently sparged into 10 mL of 40% reverse aqua regia solution (v/v, $2HNO_3$/1HCl). For the IC traps, a modified AMA catalyst tube (Leco Inc.) was utilized to retain iodine vapors produced during combustion and minimize the carry-over of iodine to the trapping solution. The AMA catalyst bed was kept at 680 °C. The recoveries of preconcentration of CLC and IC traps were investigated by combusting standard reference material BCR 482 (lichen, 480 ng $g^{-1}$) and IC traps preloaded with given amount of injected $Hg^0$ vapor (35.5 ng), respectively. Mean recoveries of combustion were 87.2 ± 2.4% (1SD, $n$ = 5) for CLC traps and 87.4 ± 2.1% (1SD, $n$ = 4) for IC traps. Full procedural blanks were determined by combustion of 600 mg of CLC and showed a mean value of 0.029 ± 0.004 ng $mL^{-1}$ ($n$ = 2), which accounted for approximately 2% of Hg concentrations in trap solutions.

After the completion of the combustion, the trapping bottles and impingers were rinsed three times with Milli-Q water. The rinsed water volume was added to trapping solutions to yield an ultimate acid concentration of 20% (v/v, $2HNO_3$/1HCl) for Hg isotopic analysis. The diluted trapping solutions were kept in a refrigerator at 4 °C until isotopic analysis. Hg concentrations in final trapping solutions were determined using a cold vapor atomic fluorescence spectroscopy (CVAFS) detection to determine the overall recovery during air TGM sampling and preconcentration.

**Mercury Isotope Analysis.** Hg isotope ratios were measured using cold vapor multicollector inductively coupled plasma mass spectrometry (CV-MC-ICPMS, Thermo-Finnigan Neptune) at the Midi-Pyrenees Observatory, Toulouse, France following the methods described in previous studies.[26,27] Instrumental mass bias of MC-ICPMS was corrected by standard−sample−standard bracketing using $NIST_{3133}$ Hg at matching concentrations. Hg isotopic composition is reported in delta notation ($\delta$) in units of per mil referenced to the


DOI: 10.1021/acs.est.6b00033
Environ. Sci. Technol. 2016, 50, 5641−5650

bracketed $NIST_{3133}$ Hg standard,[28] which is obtained using the following equation:

$$\delta^{xxx}\mathrm{Hg} = \left( \frac{\left(\frac{^{xxx}\mathrm{Hg}}{^{198}\mathrm{Hg}}\right)_{\mathrm{sample}}}{\left(\frac{^{xxx}\mathrm{Hg}}{^{198}\mathrm{Hg}}\right)_{\mathrm{SRM3133}}} - 1 \right) \times 1000‰ \quad (1)$$

MIF values are expressed by "capital delta (Δ)" notation (‰), which is the difference between the measured values of $\delta^{199}$Hg, $\delta^{200}$Hg, and $\delta^{201}$Hg and those predicted from $\delta^{202}$Hg using the kinetic MDF law:[28]

$$\Delta^{199}\mathrm{Hg}\ (‰) = \delta^{199}\mathrm{Hg} - (0.252 \times \delta^{202}\mathrm{Hg}) \quad (2)$$

$$\Delta^{200}\mathrm{Hg}\ (‰) = \delta^{200}\mathrm{Hg} - (0.502 \times \delta^{202}\mathrm{Hg}) \quad (3)$$

$$\Delta^{201}\mathrm{Hg}\ (‰) = \delta^{201}\mathrm{Hg} - (0.752 \times \delta^{202}\mathrm{Hg}) \quad (4)$$

$$\Delta^{204}\mathrm{Hg}\ (‰) = \delta^{204}\mathrm{Hg} - (1.493 \times \delta^{202}\mathrm{Hg}) \quad (5)$$

Analytical uncertainty of isotopic analysis was obtained by repeated analysis of the UM-Almaden standard ($n$ = 11) over different analysis. The overall mean values of $\delta^{202}$Hg, $\Delta^{199}$Hg, $\Delta^{200}$Hg, $\Delta^{201}$Hg, and $\Delta^{204}$Hg for all the UM-Almaden standards were −0.52 ± 0.07 ‰, −0.02 ± 0.08‰, −0.01 ± 0.09 ‰, −0.05 ± 0.09 ‰, and 0.04 ± 0.19 ‰ (2SD, $n$ = 11), respectively, which agree well with previously reported values.[28] In the present study, the analytical uncertainty of CV-MC-ICPMS isotope analysis is the 2SD uncertainty of the UM-Almaden standard, unless the 2SD uncertainty on repeated analysis of the same sample over different analytical sessions is larger.

**Ancillary Parameters.** Atmospheric Hg speciation including GEM, GOM, and PBM was continuously measured using the Tekran 2537B/1130/1135 system (Tekran Inc., Canada). GOM, PBM, and GEM in ambient air were collected onto KCl-coated annular denuder, quartz fiber filter, and dual gold cartridges in sequence. This system was programmed to collect GOM and PBM at 1 h intervals at a volumetric flow rate of 10 L $min^{-1}$; GEM was collected at 5 min intervals at a volumetric flow rate of 1.07 L $min^{-1}$. Once collected, Hg is thermally decomposed from each unit and detected by CVAFS as $Hg^0$. KCl-coated denuder, Teflon-coated glass inlet, and impactor plate were replaced biweekly, and quartz filters were replaced monthly. Denuders and quartz filters were prepared and cleaned before field sampling following the methods in Tekran technical notes. The Tekran 2537B analyzer was routinely calibrated using its internal permeation source at a 47 h interval and was also cross-calibrated every 3 months against an external temperature-controlled vapor standard. Ambient air was introduced into the Tekran unit using the Tekran 1104 manifold, and the full blanks of Tekran unit and manifold were quantified at the beginning and end of each maintenance (biweekly) using Hg-free air. The annual mean GEM blank of the Tekran unit was 0.05 ± 0.04 ng $m^{-3}$ (1SD). The sampling flow rate of Tekran 2537B analyzer was measured using a Bios Defender (Mesalabs, United States) in August 2011, February 2012, and December 2012 and showed a negligible bias (1.2%) with the flow rate setting (0.7 L $min^{-1}$ at a standard pressure of 1013 hPa and a standard temperature of 273.14 K) of the Tekran 2537B analyzer.

Automated GOM and PBM analyses are subject to mounting criticism because the techniques lack calibration, collection efficiency control, and interference correction.[3] Previous field and laboratory studies suggested that GOM concentrations measured by KCl-coated denuder could be biased low depending on chemical composition of GOM and environmental setting (e.g., ozone, relative humidity).[3,29−31] This could be due to the incomplete collection of GOM by and release of GOM compounds on KCl-coated denuder as well as deposition of GOM onto sampling Teflon tubing and biased integration of small Hg loads.[29,31−33] Preliminary observations (from July to December 2014, $n$ = 20) of manually sampled GOM+PBM fractions on cation exchange membranes (CEM) at the PDM Observatory[34] showed that our denuder-based GOM data are systematically underestimated by a factor of 2 (Marusczak et al., manuscript under preparation). This value is similar to the factors (1.6−2.4) reported for specific GOM compounds of $HgCl_2$ and $HgBr_2$ but significantly lower compared to that of HgO and $Hg(NO_3)_2$,[3,34] indicating $HgCl_2$ and $HgBr_2$ might be important specific forms of atmospheric GOM at the PDM Observatory. No clear influence of $O_3$ and relative humidity was observed on the collection efficiency of GOM by CEM relative to the Tekran system. We therefore consider our GOM and PBM observations in this study of a qualitative nature. Relative to GOM and PBM, measurements of GEM are thought to have less analytical uncertainty. Previous intercomparison of GEM concentrations measured by colocated Tekran Instruments and manual collection system generally showed average bias of less than 10%,[4,35,36] in extreme cases up to 30%.[29] Atmospheric CO and $O_3$ concentrations were continuously measured using the TEI 48CTL gas filter correlation analyzers and 49C $O_3$ instruments (Thermo Environmental Instruments Inc., United States), respectively. Detailed information regarding the principle of the CO and $O_3$ instruments, calibrations, and measurement uncertainties can be found in a previous study.[37] The standard uncertainties associated with CO and $O_3$ data sets (15 min averaged data) were reported to be 6.6 and 1.2 ppb, respectively.[37] The 5 min meteorological parameters at the PDM observatory were obtained from the PAES (French acronym for atmospheric pollution at synoptic scale) network which used standard instruments (more details are available at http://p2oa.aero.obs-mip.fr/spip.php?rubrique135).

**Air Mass Backward Trajectories.** To identify the sources and pathway of air masses associated with atmospheric TGM isotopes, 3 day backward HYSPLIT isentropic trajectories ending at PDM at a height of 3000 m above sea level (approximately 100 m above the sampling site) were simulated. Backward trajectories of the biweekly samples were calculated every 2 h using the TrajStat Geographical Information System-based software and gridded meteorological data (Global Data Assimilation System, GDAS1) from the U.S. National Oceanic and Atmospheric Administration (NOAA).[38] The gridded meteorological data covered a 360 × 180 deg latitude−longitude domain with a horizontal resolution of 1 × 1 degree latitude/longitude and vertical levels of 23 from 1000 hPa to 20 hPa. Atmospheric air mass residence times in a regular 0.5° × 0.5° grid cell (ARTs, total number of backward trajectory segment end points in a grid cell) for each biweekly period were calculated from the 3 day backward trajectories ending at PDM. The 3 day backward trajectories mainly (~92%) covered the Europe and the North Atlantic Ocean, which is slightly higher than that (~80%) of 7 day backward trajectories. The locations of air sources simulated by the trajectory generally have a larger uncertainty as trajectory running time increases.[39]



DOI: 10.1021/acs.est.6b00033
Environ. Sci. Technol. 2016, 50, 5641−5650

Also, signatures of atmospheric Hg speciation and isotopes of air masses from distant regions could be confounded during long-range atmospheric transport. We therefore deem that 3 day backward trajectories are appropriate to probe the effect of air masses from the Europe and North Atlantic Ocean on the atmospheric TGM isotope compositions and atmospheric Hg speciation.

## RESULTS AND DISCUSSION

**Hg Speciation Dynamics.** Average GEM, GOM, and PBM concentrations during the study period (February 13, 2012 to January 25, 2013) were 1.85 ng $m^{-3}$, 34 pg $m^{-3}$, and 14 pg $m^{-3}$, respectively (Table S1 of the Supporting Information). GEM concentrations at PDM were relatively higher than those observed at high- and low-altitude sites in North America, Europe, and Taiwan (1.54−1.73 ng $m^{-3}$)[19−21,40,41] but lower than those observed at high-altitude sites in mainland China (1.98−2.80 ng $m^{-3}$).[42−44] Elevated GEM concentrations at PDM were likely caused by contributions from GEM enriched boundary layer air. The GOM levels were within the range of values reported for high-altitude sites (19−43 pg $m^{-3}$)[19−21,23,43] but significantly higher than GOM observed at low-altitude sites globally.[45]

**TGM Isotopic Composition: QA/QC.** Atmospheric TGM was collected as 25 biweekly integrated samples from February 13, 2012 to January 25, 2013. TGM isotopic compositions, GEM, GOM, CO, and $O_3$ concentrations as well as the overall recovery of isotopic samples during the study period are summarized in Table S1. Recoveries of the biweekly samples ranged from 77% to 105% with a mean of 89 ± 6% (1SD, $n$ = 25). The mean 11% bias in the overall recoveries could have resulted from small losses during biweekly collection of atmospheric TGM, carbon trap desorption, and analytical uncertainties of the CVAFS analysis and Tekran 2537B/1130/1135 system. Overall, the mean recovery of biweekly samples was comparable to those obtained from the combustion of IC and CLC traps with known amounts of Hg (mean: 87%, $n$ = 9),[25] indicating that the loss of TGM during sample collection and processing was minor. Additionally, duplicate biweekly sampling did not show significant differences in MDF and MIF of Hg isotopes (e.g., paired sample $t$ test, $p_{\delta^{202}Hg}$ = 0.29, $p_{\Delta^{199}Hg}$= 0.43, $n$ = 6).

**GEM Isotope Compositions.** Mountaintop observations of GOM in the free troposphere can be as high as 500 pg $m^{-3}$, in which case GOM makes up a substantial fraction of TGM.[19,46] For this study it therefore is important to discuss if the TGM isotopic composition represents the GEM isotopic composition and at what point it becomes confounded by the partially cocollected GOM isotopic composition. Under the biweekly sampling conditions, and based on KCl-coated denuder sampling, the GOM fraction is on average 1.8% of TGM and never exceeds 4.5% (sample B18). Huang et al. observed that GOM collection by KCl-coated denuders is 1.3−3.7 times lower than by cation exchange membranes.[34] Preliminary observations of manually sampled GOM+PBM fractions on cation exchange membranes (CEMs) at PDM shows that our denuder-based GOM data are systematically underestimated by a factor of 2. The average GOM fraction could therefore represent up to 3.6% of TGM and temporarily up to 9% (sample B18). Observations on rainfall, which scavenges GOM and PBM, collected in the Pyrenees show average $\delta^{202}$Hg and $\Delta^{199}$Hg of −0.5‰ and 0.4‰, respectively.[47] Mean biweekly integrated $\delta^{202}Hg_{TGM}$ and $\Delta^{199}Hg_{TGM}$ in this study was 0.19‰ and −0.21‰, respectively. A worst case 3.6−9% GOM contribution to TGM would therefore not have measurably shifted the $\delta^{202}Hg_{TGM}$ and $\Delta^{199}Hg_{TGM}$ values. The biweekly sample (sample B18) with highest GOM fraction (4.5%) incidentally also had the highest $\delta^{202}Hg_{TGM}$ (0.38‰) and is therefore shifted in the opposite direction from what one would expect from a GOM contribution to TGM. We therefore deem GOM confounding of TGM insignificant in the biweekly samples and interpret the TGM observations as GEM isotopic compositions, i.e., $\delta^{202}Hg_{GEM}$, $\Delta^{199}Hg_{GEM}$, $\Delta^{200}Hg_{GEM}$, and $\Delta^{204}Hg_{GEM}$.

Hg isotope compositions of biweekly samples at PDM ($n$ = 27) varied from −0.04 to 0.52‰ ($\delta^{202}Hg_{GEM}$), −0.17 to −0.27‰ ($\Delta^{199}Hg_{GEM}$), −0.10 to 0.05‰ ($\Delta^{200}Hg_{GEM}$), −0.26 to −0.18‰ ($\Delta^{201}Hg_{GEM}$), and −0.03 to 0.14‰ ($\Delta^{204}Hg_{GEM}$) during the one-year period (Table S1). The isotopic compositions of atmospheric GEM at PDM were overall consistent with observations at low-altitude remote sites. $\delta^{202}Hg_{GEM}$ measurements at PDM were comparable to those of the Great Lakes region, United States ($\delta^{202}Hg_{TGM}$ = 0.27 to 0.43‰)[15] and to two samples from Barrow, Alaska ($\delta^{202}Hg_{TGM}$ = −0.12‰ and 0.15‰)[14] but slightly lower than those measured at the top of a forest canopy in rural Wisconsin, United States ($\delta^{202}Hg_{TGM}$ = 0.48 to 0.93‰) and in an open field in Pensacola, FL, United States ($\delta^{202}Hg_{TGM}$ = 0.39 to 1.43‰).[12,18] $\Delta^{199}Hg_{GEM}$ values at PDM (−0.27 to −0.17‰) were slightly lower than those observed in the Great Lakes region ($\Delta^{199}Hg_{TGM}$ = −0.14 to −0.01‰)[15] but similar to those measured in Barrow (−0.11 to −0.22‰), the Wisconsin forest canopy (−0.15 to −0.21‰), and Pensacola, FL, United States (−0.11 to −0.31‰).[12,14,18] On the other hand, isotopic compositions of atmospheric GEM at PDM were more different from observations in urban Chicago, United States, which is heavily impacted by industrial sources ($\delta^{202}Hg_{TGM}$ = −0.58‰, $\Delta^{199}Hg_{TGM}$ = 0.06‰).[15] $\Delta^{200}Hg_{TGM}$ (and $\Delta^{204}Hg_{TGM}$) was similar and near zero across all studies. All of the cited studies and this study have very different $\delta^{202}Hg_{TGM}$ from a study on coastal TGM in Grand Bay, Mississippi, United States (mean $\delta^{202}Hg_{TGM}$ = −2.7‰).[17] A recent TGM isotope study in Pensacola (FL, United States), 130 km east of Grand Bay, did not reproduce the highly negative $\delta^{202}Hg_{TGM}$.[18] Apart from the Grand Bay study, global TGM observations indicate a significant variation in $\delta^{202}$Hg (−0.6‰ to 1.43‰) and $\Delta^{199}$Hg (−0.31‰ to 0.06‰) (Figure S1).

**Annual Trends in Biweekly $\delta^{202}Hg_{GEM}$ and $\Delta^{199}Hg_{GEM}$.** A significant seasonal variation in $\delta^{202}Hg_{GEM}$ was observed throughout the whole sampling period ($p$ < 0.05, Figure 1a, Table S1). The $\delta^{202}Hg_{GEM}$ in February and March 2012 ranged from −0.04 ‰ to 0.01 ‰ and was approximately 0.1−0.2 ‰ lower compared to $\delta^{202}$Hg values in April and May 2012. Air masses in February and March 2012 mainly originated from and passed over central Europe, carried by cold northeastern winds, whereas air masses in April and May of 2012 originated from and passed over the North Atlantic Ocean and mountainous areas of the Pyrenees (Figure S2). $\delta^{202}Hg_{GEM}$ in June and August 2012 were in the range of −0.02 ‰ to 0.18 ‰ and were mainly influenced by polluted, high CO air masses that passed over Spain (Figures 1b and S1). GEM collected from December 2012 to January 2013 represents low CO air masses from the North Atlantic Ocean (mild 2013 winter) and was characterized by relatively high $\delta^{202}Hg_{GEM}$ values compared to other periods (Figure 1a, with the highest $\delta^{202}Hg_{GEM}$ of 0.52 ‰ in January 2013). Fractional atmospheric air mass residence


DOI: 10.1021/acs.est.6b00033
Environ. Sci. Technol. 2016, 50, 5641−5650

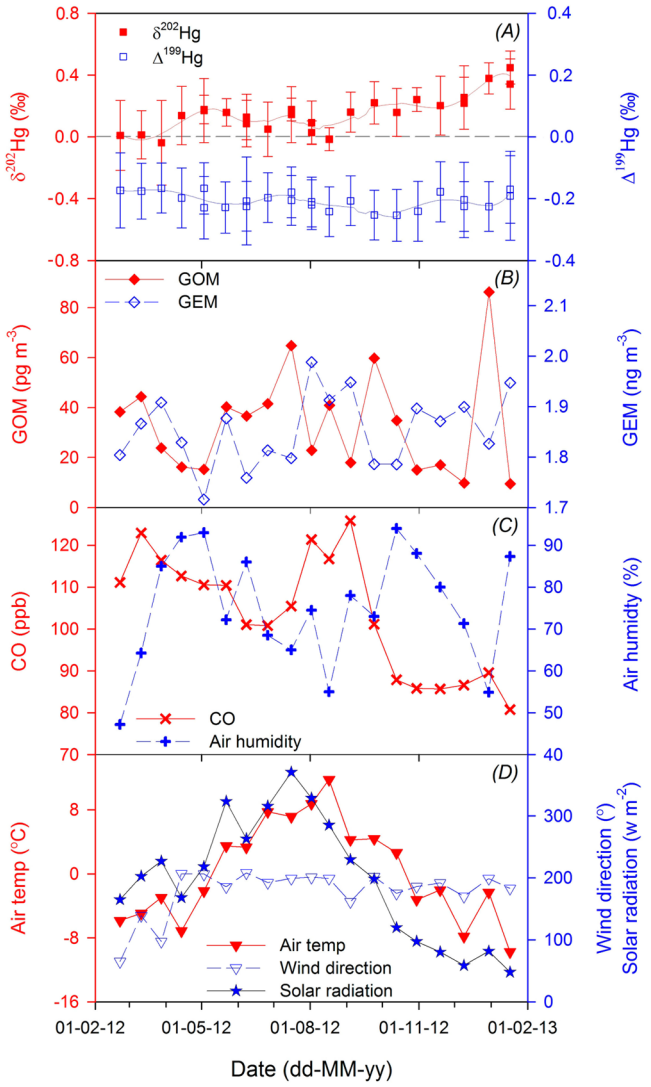


**Figure 1.** Annual temporal variation in (A) atmospheric GEM $\Delta^{199}$Hg and $\delta^{202}$Hg for biweekly samples (error bar on GEM $\Delta^{199}$Hg and $\delta^{202}$Hg data indicates 2SD uncertainty); (B) atmospheric GOM and GEM concentrations; (C) CO concentrations and relative humidity; and (D) air temperature, solar radiation, and wind direction.

times (ARTs) were estimated from 3 day backward trajectories, i.e., the percent of time an air mass spent over Europe or over the North Atlantic Ocean during the three preceding days. Fractional European ARTs were negatively correlated with $\delta^{202}Hg_{GEM}$ ($r^2 = 0.29$, $p < 0.01$) while Fractional North Atlantic ARTs were positively correlated with $\delta^{202}Hg_{GEM}$ ($r^2 = 0.35$, $p < 0.01$) (Figure S3). Extrapolating fractional ARTs to 0% and 100% suggests that the approximate North Atlantic Ocean and continental European air mass end-members have $\delta^{202}Hg_{GEM}$ of 0.43‰ and −0.13 ‰, respectively.

A significant negative linear correlation was observed between $\delta^{202}Hg_{GEM}$ and CO concentrations during the study period (Figure 2). No significant relationship existed between $\delta^{202}Hg_{GEM}$ and GEM, PBM, $O_3$, air temperature, wind direction, and relative humidity ($p$ values for all >0.05). CO in the atmosphere is mainly derived from fossil fuel combustion and biomass burning, and CO emitted from the oceans is negligible in the global atmospheric CO budget.[48] In Europe, natural emissions of CO are lower than anthropogenic emissions.[49] The strong negative correlation between CO and

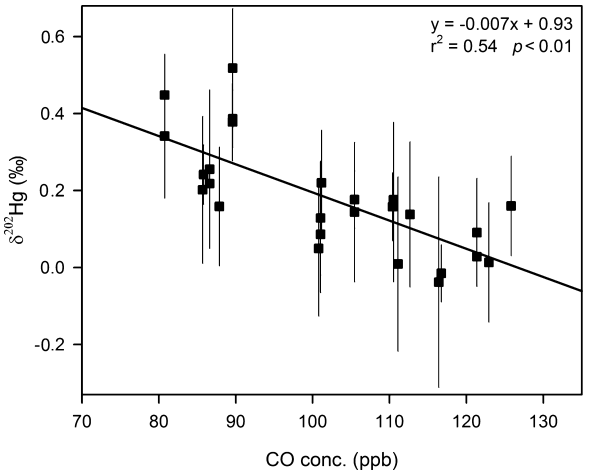


**Figure 2.** Relationship between CO levels and GEM $\delta^{202}$Hg for all atmospheric samples (error bar on GEM $\delta^{202}$Hg data indicates 2SD uncertainty).

$\delta^{202}Hg_{GEM}$, as well as the back trajectory and ARTs analysis, indicates that GEM in continental European air masses is characterized by $\delta^{202}Hg_{GEM}$ values lower than those of the North Atlantic Ocean free troposphere. Biweekly variations in $\Delta^{199}Hg_{GEM}$, $\Delta^{200}Hg_{GEM}$, $\Delta^{201}Hg_{GEM}$, and $\Delta^{204}Hg_{GEM}$ were not significantly different from the annual mean for the 1 year study period ($p$ values for all >0.05; Figure 1, Table S1). Consequently, no clear relationship can be established between biweekly odd-MIF and even-MIF signatures and transport of air masses or atmospheric processes.

The challenge is therefore to understand why European air masses have lower $\delta^{202}Hg_{GEM}$, but similar MIF as Atlantic Ocean air masses. An oceanic air mass does not necessarily contain a larger amount or fraction of natural Hg than a continental air mass. Amos et al. estimate that preanthropogenic (<2000 BC) atmospheric GEM levels were on the order of 0.2 ng $m^{-3}$ or less.[50,51] The Atlantic Ocean and European continental air masses observed both had mean GEM of 1.85 ng $m^{-3}$. Therefore, both air masses contain >90% of Hg from anthropogenic origins. This notion is also reflected in a comparison of modern-day natural, anthropogenic, and legacy Hg emissions. Recent observational and modeling constraints on natural volcanic Hg emissions suggest a 76−90 Mg $y^{-1}$ flux,[52,53] which is an order of magnitude smaller than global anthropogenic Hg emissions of 2000 Mg $y^{-1}$.[6] The latter, however, is a factor of 2 smaller than the ∼4700 Mg $y^{-1}$ combined oceanic and continental re-emission of predominantly legacy Hg.[54] Similar emissions can be estimated at the regional scale: North American (predominantly United States) and European anthropogenic Hg emissions are on the order of 61 and 88 Mg $y^{-1}$, respectively, while North Atlantic Ocean and European soil Hg re-emissions are approximately 300 and 154 Mg $y^{-1}$, respectively (global fluxes scaled for Atlantic and Europe surface areas).[6] On both a global and regional scale, primary anthropogenic Hg emissions are therefore significant though smaller than re-emission of legacy Hg.

The mean of global $\delta^{202}Hg_{TGM}$ (0.52 ± 0.40‰, 1SD; data are from the present study and the literature),[12,15,18] is significantly more positive than the $\delta^{202}$Hg of industrial source materials such as coal (−1.24 ± 0.87‰, 1SD) or cinnabar (−0.59 ± 0.30‰, 1SD) (Figure 3).[55,56] Recent studies suggested that the positive $\delta^{202}Hg_{GEM}$ shift is potentially due


DOI: 10.1021/acs.est.6b00033
Environ. Sci. Technol. 2016, 50, 5641−5650

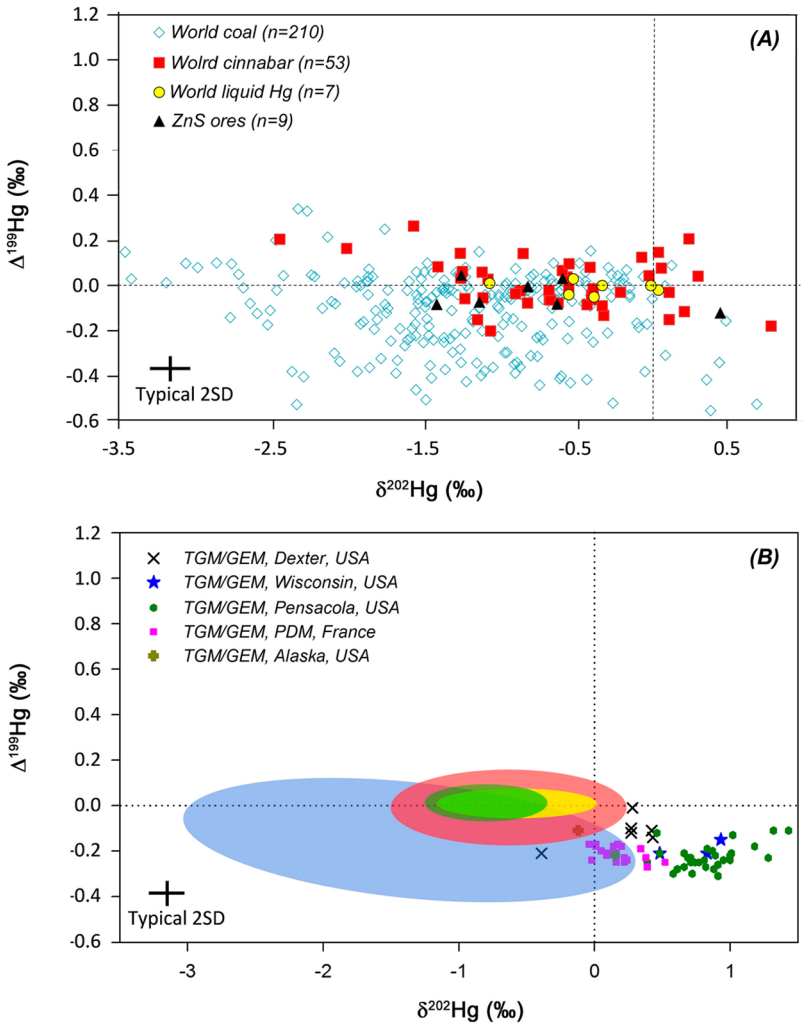


**Figure 3.** Hg mass-dependent ($\delta^{202}$Hg) and mass-independent ($\Delta^{199}$Hg) isotope signatures in anthropogenic and natural emission sources (A) and in atmospheric total gaseous Hg (B; TGM, filled symbols). The dotted lines indicate zero-values for $\delta^{202}$Hg and $\Delta^{199}$Hg. The shaded areas in panel B correspond approximately to the emissions sources in panel A, i.e., coal (blue), HgS and ZnS (red), liquid Hg (yellow), and volcanic TGM (green). Data are from this study and the literature.[7,12,14−16,18,58,67−71]

to a combination of heavy isotope enriched industrial GEM emissions and light isotope enrichment during foliar uptake of GEM.[12,47,57] In the following we will therefore consider the following factors to interpret the $\delta^{202}Hg_{GEM}$ variations observed at PDM: (1) $\delta^{202}Hg_{GEM}$ of anthropogenic emissions and the proximity of emission sources to PDM and (2) MDF during Hg transformations at the interface of earth surface environments and the atmosphere.

**Hg Source versus Hg Transformation Control on MDF.** Modern-day anthropogenic Hg emissions from nothern hemispheric continents (Asia, North America, Europe, and Russia) are dominated by Hg emissions from coal-fired power plants and coal-consuming industries (metallurgy, cement).[1,2] Sun et al. recently documented and compiled Hg isotope signatures of >200 world coal deposits and discussed $\delta^{202}$Hg and $\Delta^{199}$Hg signatures of GEM emissions from coal burning.[58] Raw coal from China, United States, Europe, and Russia have $\delta^{202}$Hg of −0.95, −1.42, −1.17, and −1.69‰ and $\Delta^{199}$Hg of 0.01, −0.10, −0.38, and −0.19‰, respectively ($n$ = 110, 27, 13, 21), and coal from all four regions can be statistically distinguished at the $p$ = 0.05 level. $\Delta^{200}$Hg in world coal deposits are all near zero. North American and European anthropogenic Hg emissions are dominated (>75%) by coal combustion if we lump together stationary combustion and coal use in the metallurgy and cement sectors.[6] Atlantic Ocean and European air masses therefore contain a non-negligible fraction of recently emitted GEM from North American (predominantly United States) and European coal combustion, respectively. If coal Hg emissions were to resemble feed coal, then North Atlantic $\delta^{202}Hg_{GEM}$, influenced by United States coal, should be lower than European $\delta^{202}Hg_{GEM}$ influenced by European coal, and vice versa for $\Delta^{199}$Hg. The observed $\delta^{202}Hg_{GEM}$ and $\Delta^{199}Hg_{GEM}$, however, show an opposite trend: Atlantic air has higher $\delta^{202}Hg_{GEM}$ than European air, and $\Delta^{199}Hg_{GEM}$ shows no variation. This interpretation, however, is too simplistic for various reasons. While United States coal data is abundant ($n$ = 27), the representativeness of the European coal sample set is doubtful, because coal data from the largest emitters, Germany, Poland, and the United Kingdom, are missing.[58] Further complications arise from European coal imports and associated $\delta^{202}$Hg and $\Delta^{199}$Hg from various regions. In 2012, Europe imported >70% of its 320 Mt hard coal consumption from Russia, United States, and Colombia, though it produced 100% of its 438 Mt lignite consumption.[59] Finally, Sun et al. suggest that emission control technology in coal-burning industries induces substantial mass-dependent Hg


DOI: 10.1021/acs.est.6b00033
Environ. Sci. Technol. 2016, 50, 5641−5650

isotope fractionation of emitted GEM, GOM, and PBM species.[57] All in all, current knowledge on anthropogenic Hg isotope emissions is insufficient to explain the observed PDM trends.

Because of the proximity of the PDM site to European industrial emission sources, the European air mass likely contains a larger fraction of recently (preceding week) emitted GEM, while the Atlantic air mass contains a larger fraction of legacy GEM that has been "processed". By "processed" we mean that the majority of Atlantic GEM may have been previously oxidized in the atmosphere, reduced in clouds and re-emitted, deposited to and re-emitted from the oceans, and deposited to and re-emitted from the continents. The sum of these transformations has likely led to a shift in Hg isotopic composition relative to the originally emitted isotope signatures. Two natural atmospheric GEM transformations in particular may increase ambient $\delta^{202}Hg_{GEM}$ in the heavier isotopes (Figure 3): (i) atmospheric oxidation and (ii) foliar uptake of GEM. Relative to global $\delta^{202}Hg_{TGM}$ (mean of 0.52 ± 0.40‰; data are from the present study and the literature),[12,15,18] observations on rainfall $\delta^{202}$Hg at nonindustrial sites (mean of −0.66 ± 0.51‰, Figure S1) suggest that atmospheric oxidized forms of Hg (GOM and PBM, scavenged by clouds and precipitation) are enriched in the lighter isotopes.[12,15,16,60] This is consistent with kinetic isotope fractionation enriching the oxidized Hg product in the lighter isotopes, leaving behind reactant GEM enriched in the heavy isotopes. Recent studies observed that foliar GEM uptake strongly enriches plant leaves (by −2.3 to −2.9‰) and soil organic matter in the lighter Hg isotopes.[12] Enrico et al. also observed an atmospheric TGM pool with $\delta^{202}$Hg up to 1.2‰ over a forested peat bog and suggested foliar uptake to be a potential driver for highly positive $\delta^{202}$Hg values in the atmospheric TGM pool.[47]

Biweekly integrated GOM concentrations also show a distinct, though complex and nonlinear, relationship with $\delta^{202}Hg_{GEM}$ (Figure 4). Elevated $\delta^{202}Hg_{GEM}$, associated with a North Atlantic origin, show both low (biweekly means of <20 pg m$^{-3}$) and high GOM levels (biweekly means of >40 pg m$^{-3}$). Previous studies have suggested that marine boundary layer (MBL) and continental free troposphere (FT) have a strong potential to oxidize GEM to GOM due to $BrO_x$- and $O_3$/HO$^{\bullet}$-induced chemical reactions.[23,46,61,62] In the present study, a significant positive correlation ($r^2$ = 0.60, $p$ < 0.01) is observed between biweekly integrated GOM concentrations and the fractional ARTs over North Atlantic free troposphere (FT), whereas no clear relationship can be established between biweekly integrated GOM concentrations and the fractional ARTs over the North Atlantic MBL, European planetary boundary layer (PBL), and European FT ($p$ values for all >0.05, Figure S4). This implies that the North Atlantic FT rather than North Atlantic MBL and European troposphere was the major source region of GOM at PDM. Enrichment of GOM in the North Atlantic FT is therefore consistent with increasing levels of atmospheric oxidants (e.g., ozone, nitrate radicals, reactive halogens) with altitude.[63−65] In addition, GOM for this elevated $\delta^{202}Hg_{GEM}$ subgroup (>0.1‰, indicating the major air source origins of North Atlantic Ocean) is inversely correlated with relative humidity ($r^2$ = 0.69, $p$ < 0.01, Figure S5), suggesting that aerosol and cloudwater scavenging control GOM concentrations but not $\delta^{202}Hg_{GEM}$. Most likely the $\delta^{202}Hg_{GEM}$ signature was acquired before GOM was scavenged. The finding that the production of GOM in the North Atlantic

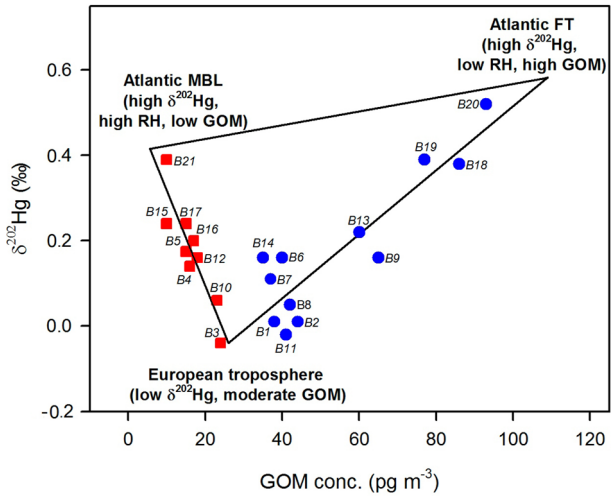


**Figure 4.** Atmospheric GOM concentrations versus GEM $\delta^{202}$Hg for biweekly samples throughout the sampling campaign and a diagram showing the three end-members [Atlantic marine boundary layer (MBL), European troposphere (ET), and Atlantic free troposphere (FT)] of potential sources of atmospheric GOM using the GEM $\delta^{202}$Hg signatures. The red squares indicate the biweekly samples mainly influenced by mixing air from the Atlantic MBL and European troposphere, and blue circles indicate the biweekly samples mainly influenced by mixing air from the European troposphere and Atlantic FT.

FT is stronger than in the European PBL and FT is possibly due to the release of halogen compounds from oceanic surfaces which are potentially important oxidants for GEM.[62,66] The persistently elevated $\delta^{202}Hg_{GEM}$ of North Atlantic air corroborates our suggestion that atmospheric oxidation depletes residual GEM in the heavier isotopes and partly drives the observed $\delta^{202}Hg_{GEM}$ variations at PDM.

## ■ ASSOCIATED CONTENT

### Supporting Information

The Supporting Information is available free of charge on the ACS Publications website at DOI: 10.1021/acs.est.6b00033.

Additional details of the isotopic compositions of atmospheric mercury, speciated atmospheric mercury concentrations, ancillary observations, and Figures S1−S5 (PDF)

## ■ AUTHOR INFORMATION

### Corresponding Authors

*Phone: +86 851 85891508; fax: +86 851 85891609; e-mail: fuxuewu@mail.gyig.ac.cn.

*Phone: +33561332606; fax: +33561332560; e-mail: jeroen.sonke@get.omp.eu.

### Notes

The authors declare no competing financial interest.

## ■ ACKNOWLEDGMENTS

This work is supported by research Grant ERC-2010-StG_20091028 from the European Research Council and the National Science Foundation of China (41473025 and 41274145). Observation data were collected at the Pyrenean Platform for Observation of the Atmosphere P2OA (http://p2oa.aero.obs-mip.fr). P2OA facilities and staff are funded and supported by the University Paul Sabatier, Toulouse, France,



DOI: 10.1021/acs.est.6b00033
Environ. Sci. Technol. 2016, 50, 5641−5650

and CNRS (Centre National de la Recherche Scientifique). We especially acknowledge technical support from the UMS 831 Pic du Midi Observatory team and from Jerome Chmeleff on the OMP Neptune. We thank Lars-Eric Heimbürger for help with AFS analyses.

## REFERENCES

(1) Pirrone, N.; Cinnirella, S.; Feng, X.; Finkelman, R. B.; Friedli, H. R.; Leaner, J.; Mason, R.; Mukherjee, A. B.; Stracher, G. B.; Streets, D. G.; Telmer, K. Global mercury emissions to the atmosphere from anthropogenic and natural sources. *Atmos. Chem. Phys.* **2010**, *10* (13), 5951−5964.

(2) Pacyna, E. G.; Pacyna, J. M.; Sundseth, K.; Munthe, J.; Kindbom, K.; Wilson, S.; Steenhuisen, F.; Maxson, P. Global emission of mercury to the atmosphere from anthropogenic sources in 2005 and projections to 2020. *Atmos. Environ.* **2010**, *44* (20), 2487−2499.

(3) Gustin, M. S.; Amos, H. M.; Huang, J.; Miller, M. B.; Heidecorn, K. Measuring and modeling mercury in the atmosphere: a critical review. *Atmos. Chem. Phys.* **2015**, *15* (10), 5697−5713.

(4) Slemr, F.; Angot, H.; Dommergue, A.; Magand, O.; Barret, M.; Weigelt, A.; Ebinghaus, R.; Brunke, E. G.; Pfaffhuber, K. A.; Edwards, G.; Howard, D.; Powell, J.; Keywood, M.; Wang, F. Comparison of mercury concentrations measured at several sites in the Southern Hemisphere. *Atmos. Chem. Phys.* **2015**, *15* (6), 3125−3133.

(5) Amos, H. M.; Jacob, D. J.; Holmes, C. D.; Fisher, J. A.; Wang, Q.; Yantosca, R. M.; Corbitt, E. S.; Galarneau, E.; Rutter, A. P.; Gustin, M. S.; Steffen, A.; Schauer, J. J.; Graydon, J. A.; Louis, V. L., St; Talbot, R. W.; Edgerton, E. S.; Zhang, Y.; Sunderland, E. M. Gas-particle partitioning of atmospheric Hg(II) and its effect on global mercury deposition. *Atmos. Chem. Phys.* **2012**, *12* (1), 591−603.

(6) AMAP/UNEP. *Technical Background Report for the Global Mercury Assessment 2013*; Arctic Monitoring and Assessment Programme, Oslo, Norway/UNEP Chemicals Branch: Geneva, Switzerland; 2013; pp vi−263.

(7) Sonke, J. E.; Blum, J. D. Advances in mercury stable isotope biogeochemistry Preface. *Chem. Geol.* **2013**, *336*, 1−4.

(8) Bergquist, B. A.; Blum, J. D. Mass-dependent and -independent fractionation of Hg isotopes by photoreduction in aquatic systems. *Science* **2007**, *318* (5849), 417−420.

(9) Kritee, K.; Barkay, T.; Blum, J. D. Mass dependent stable isotope fractionation of mercury during *mer* mediated microbial degradation of monomethylmercury. *Geochim. Cosmochim. Acta* **2009**, *73* (5), 1285−1296.

(10) Zheng, W.; Foucher, D.; Hintelmann, H. Mercury isotope fractionation during volatilization of Hg(0) from solution into the gas phase. *J. Anal. At. Spectrom.* **2007**, *22* (9), 1097−1104.

(11) Yang, L.; Sturgeon, R. Isotopic fractionation of mercury induced by reduction and ethylation. *Anal. Bioanal. Chem.* **2009**, *393* (1), 377−385.

(12) Demers, J. D.; Blum, J. D.; Zak, D. R. Mercury isotopes in a forested ecosystem: Implications for air-surface exchange dynamics and the global mercury cycle. *Global Biogeochem Cy* **2013**, *27* (1), 222−238.

(13) Zheng, W.; Hintelmann, H. Mercury isotope fractionation during photoreduction in natural water is controlled by its Hg/DOC ratio. *Geochim. Cosmochim. Acta* **2009**, *73* (22), 6704−6715.

(14) Sherman, L. S.; Blum, J. D.; Johnson, K. P.; Keeler, G. J.; Barres, J. A.; Douglas, T. A. Mass-independent fractionation of mercury isotopes in Arctic snow driven by sunlight. *Nat. Geosci.* **2010**, *3* (3), 173−177.

(15) Gratz, L. E.; Keeler, G. J.; Blum, J. D.; Sherman, L. S. Isotopic composition and fractionation of mercury in Great Lakes precipitation and ambient air. *Environ. Sci. Technol.* **2010**, *44* (20), 7764−7770.

(16) Chen, J. B.; Hintelmann, H.; Feng, X. B.; Dimock, B. Unusual fractionation of both odd and even mercury isotopes in precipitation from Peterborough, ON, Canada. *Geochim. Cosmochim. Acta* **2012**, *90*, 33−46.

(17) Rolison, J. M.; Landing, W. M.; Luke, W.; Cohen, M.; Salters, V. J. M. Isotopic composition of species-specific atmospheric Hg in a coastal environment. *Chem. Geol.* **2013**, *336*, 37−49.

(18) Demers, J. D.; Sherman, L. S.; Blum, J. D.; Marsik, F. J.; Dvonch, J. T. Coupling atmospheric mercury isotope ratios and meteorology to identify sources of mercury impacting a coastal urban-industrial region near Pensacola, Florida, USA. *Global Biogeochem Cy* **2015**, *29* (10), 1689−1705.

(19) Swartzendruber, P. C.; Jaffe, D. A.; Prestbo, E. M.; Weiss-Penzias, P.; Selin, N. E.; Park, R.; Jacob, D. J.; Strode, S.; Jaegle, L. Observations of reactive gaseous mercury in the free troposphere at the Mount Bachelor Observatory. *J. Geophys. Res.* **2006**, *111*, D24301.

(20) Fain, X.; Obrist, D.; Hallar, A. G.; Mccubbin, I.; Rahn, T. High levels of reactive gaseous mercury observed at a high elevation research laboratory in the Rocky Mountains. *Atmos. Chem. Phys.* **2009**, *9* (20), 8049−8060.

(21) Sheu, G. R.; Lin, N. H.; Wang, J. L.; Lee, C. T.; Yang, C. F. O.; Wang, S. H. Temporal distribution and potential sources of atmospheric mercury measured at a high-elevation background station in Taiwan. *Atmos. Environ.* **2010**, *44* (20), 2393−2400.

(22) Lyman, S. N.; Jaffe, D. A. Formation and fate of oxidized mercury in the upper troposphere and lower stratosphere. *Nat. Geosci.* **2012**, *5* (2), 114−117.

(23) Brooks, S.; Ren, X. R.; Cohen, M.; Luke, W. T.; Kelley, P.; Artz, R.; Hynes, A.; Landing, W.; Martos, B. Airborne vertical profiling of mercury speciation near Tullahoma, TN, USA. *Atmosphere* **2014**, *5* (3), 557−574.

(24) Henne, S.; Brunner, D.; Folini, D.; Solberg, S.; Klausen, J.; Buchmann, B. Assessment of parameters describing representativeness of air quality in-situ measurement sites. *Atmos. Chem. Phys.* **2010**, *10* (8), 3561−3581.

(25) Fu, X. W.; Heimburger, L. E.; Sonke, J. E. Collection of atmospheric gaseous mercury for stable isotope analysis using iodine- and chlorine-impregnated activated carbon traps. *J. Anal. At. Spectrom.* **2014**, *29* (5), 841−852.

(26) Sun, R. Y.; Enrico, M.; Heimburger, L. E.; Scott, C.; Sonke, J. E. A double-stage tube furnace-acid-trapping protocol for the pre-concentration of mercury from solid samples for isotopic analysis. *Anal. Bioanal. Chem.* **2013**, *405* (21), 6771−6781.

(27) Sonke, J. E.; Zambardi, T.; Toutain, J. P. Indirect gold trap-MC-ICP-MS coupling for Hg stable isotope analysis using a syringe injection interface. *J. Anal. At. Spectrom.* **2008**, *23* (4), 569−573.

(28) Blum, J. D.; Bergquist, B. A. Reporting of variations in the natural isotopic composition of mercury. *Anal. Bioanal. Chem.* **2007**, *388* (2), 353−359.

(29) Gustin, M. S.; Huang, J. Y.; Miller, M. B.; Peterson, C.; Jaffe, D. A.; Ambrose, J.; Finley, B. D.; Lyman, S. N.; Call, K.; Talbot, R.; Feddersen, D.; Mao, H. T.; Lindberg, S. E. Do we understand what the mercury speciation instruments are actually measuring? Results of RAMIX. *Environ. Sci. Technol.* **2013**, *47* (13), 7295−7306.

(30) McClure, C. D.; Jaffe, D. A.; Edgerton, E. S. Evaluation of the KCl denuder method for gaseous oxidized mercury using $HgBr_2$ at an In-Service AMNet Site. *Environ. Sci. Technol.* **2014**, *48* (19), 11437−11444.

(31) Huang, J. Y.; Gustin, M. S. Uncertainties of gaseous oxidized mercury measurements using KCl-coated denuders, Cation-exchange membranes, and Nylon membranes: Humidity influences. *Environ. Sci. Technol.* **2015**, *49* (10), 6102−6108.

(32) Lyman, S. N.; Jaffe, D. A.; Gustin, M. S. Release of mercury halides from KCl denuders in the presence of ozone. *Atmos. Chem. Phys.* **2010**, *10* (17), 8197−8204.

(33) Slemr, F.; Weigelt, A.; Ebinghaus, R.; Kock, H. H.; Bödewadt, J.; Brenninkmeijer, C. A. M.; Rauthe-Schöch, A.; Weber, S.; Hermann, M.; Zahn, A.; Martinsson, B. Atmospheric mercury measurements onboard the CARIBIC passenger aircraft. *Atmos. Meas. Tech.* **2016**, *9*, 2291−2302.

(34) Huang, J. Y.; Miller, M. B.; Weiss-Penzias, P.; Gustin, M. S. Comparison of gaseous oxidized Hg measured by KCl-coated



DOI: 10.1021/acs.est.6b00033
*Environ. Sci. Technol.* 2016, 50, 5641−5650

denuders, and Nylon and Cation exchange Membranes. *Environ. Sci. Technol.* **2013**, *47* (13), 7307−7316.
(35) Ebinghaus, R.; Jennings, S. G.; Schroeder, W. H.; Berg, T.; Donaghy, T.; Guentzel, J.; Kenny, C.; Kock, H. H.; Kvietkus, K.; Landing, W.; Muhleck, T.; Munthe, J.; Prestbo, E. M.; Schneeberger, D.; Slemr, F.; Sommar, J.; Urba, A.; Wallschlager, D.; Xiao, Z. International field intercomparison measurements of atmospheric mercury species at Mace Head, Ireland. *Atmos. Environ.* **1999**, *33* (18), 3063−3073.
(36) Lyman, S. N.; Gustin, M. S.; Prestbo, E. M.; Marsik, F. J. Estimation of dry deposition of atmospheric mercury in Nevada by direct and indirect methods. *Environ. Sci. Technol.* **2007**, *41* (6), 1970−1976.
(37) Gheusi, F.; Ravetta, F.; Delbarre, H.; Tsamalis, C.; Chevalier-Rosso, A.; Leroy, C.; Augustin, P.; Delmas, R.; Ancellet, G.; Athier, G.; Bouchou, P.; Campistron, B.; Cousin, J. M.; Fourmentin, M.; Meyerfeld, Y. Pic 2005, a field campaign to investigate low-tropospheric ozone variability in the Pyrenees. *Atmos. Res.* **2011**, *101* (3), 640−665.
(38) Wang, Y. Q.; Zhang, X. Y.; Draxler, R. R. TrajStat: GIS-based software that uses various trajectory statistical analysis methods to identify potential sources from long-term air pollution measurement data. *Environ. Modell Softw* **2009**, *24* (8), 938−939.
(39) Engstrom, A.; Magnusson, L. Estimating trajectory uncertainties due to flow dependent errors in the atmospheric analysis. *Atmos. Chem. Phys.* **2009**, *9* (22), 8857−8867.
(40) Lan, X.; Talbot, R.; Castro, M.; Perry, K.; Luke, W. Seasonal and diurnal variations of atmospheric mercury across the US determined from AMNet monitoring data. *Atmos. Chem. Phys.* **2012**, *12* (21), 10569−10582.
(41) Weigelt, A.; Ebinghaus, R.; Manning, A. J.; Derwent, R. G.; Simmonds, P. G.; Spain, T. G.; Jennings, S. G.; Slemr, F. Analysis and interpretation of 18 years of mercury observations since 1996 at Mace Head, Ireland. *Atmos. Environ.* **2015**, *100*, 85−93.
(42) Fu, X. W.; Feng, X.; Dong, Z. Q.; Yin, R. S.; Wang, J. X.; Yang, Z. R.; Zhang, H. Atmospheric gaseous elemental mercury (GEM) concentrations and mercury depositions at a high-altitude mountain peak in south China. *Atmos. Chem. Phys.* **2010**, *10* (5), 2425−2437.
(43) Fu, X. W.; Feng, X.; Liang, P.; Deliger; Zhang, H.; Ji, J.; Liu, P. Temporal trend and sources of speciated atmospheric mercury at Waliguan GAW station, Northwestern China. *Atmos. Chem. Phys.* **2012**, *12* (4), 1951−1964.
(44) Zhang, H.; Fu, X. W.; Lin, C.-J.; Wang, X.; Feng, X. B. Observation and analysis of speciated atmospheric mercury in Shangri-La, Tibetan Plateau, China. *Atmos. Chem. Phys.* **2015**, *15*, 653−665.
(45) Valente, R. J.; Shea, C.; Humes, K. L.; Tanner, R. L. Atmospheric mercury in the Great Smoky Mountains compared to regional and global levels. *Atmos. Environ.* **2007**, *41* (9), 1861−1873.
(46) Timonen, H.; Ambrose, J. L.; Jaffe, D. A. Oxidation of elemental Hg in anthropogenic and marine airmasses. *Atmos. Chem. Phys.* **2013**, *13* (5), 2827−2836.
(47) Enrico, M.; Roux, G. L.; Marusczak, N.; Heimbürger, L.-E.; Claustres, A.; Fu, X.; Sun, R.; Sonke, J. E. Atmospheric mercury transfer to peat bogs dominated by gaseous elemental mercury dry deposition. *Environ. Sci. Technol.* **2016**, *50* (5), 2405−2412.
(48) Holloway, T.; Levy, H.; Kasibhatla, P. Global distribution of carbon monoxide. *J. Geophys Res-Atmos* **2000**, *105* (D10), 12123−12147.
(49) Hooghiemstra, P. B.; Krol, M. C.; Meirink, J. F.; Bergamaschi, P.; van der Werf, G. R.; Novelli, P. C.; Aben, I.; Rockmann, T. Optimizing global CO emission estimates using a four-dimensional variational data assimilation system and surface network observations. *Atmos. Chem. Phys.* **2011**, *11* (10), 4705−4723.
(50) Amos, H. M.; Jacob, D. J.; Streets, D. G.; Sunderland, E. M. Legacy impacts of all-time anthropogenic emissions on the global mercury cycle. *Global Biogeochem Cy* **2013**, *27* (2), 410−421.
(51) Amos, H. M.; Jacob, D. J.; Kocman, D.; Horowitz, H. M.; Zhang, Y. X.; Dutkiewicz, S.; Horvat, M.; Corbitt, E. S.; Krabbenhoft, D. P.; Sunderland, E. M. Global biogeochemical implications of mercury discharges from rivers and sediment burial. *Environ. Sci. Technol.* **2014**, *48* (16), 9514−9522.
(52) Amos, H. M.; Sonke, J. E.; Obrist, D.; Robins, N.; Hagan, N.; Horowitz, H. M.; Mason, R. P.; Witt, M.; Hedgecock, I. M.; Corbitt, E. S.; Sunderland, E. M. Observational and modeling constraints on global anthropogenic enrichment of mercury. *Environ. Sci. Technol.* **2015**, *49* (7), 4036−4047.
(53) Bagnato, E.; Barra, M.; Cardellini, C.; Chiodini, G.; Parello, F.; Sprovieri, M. First combined flux chamber survey of mercury and $CO_2$ emissions from soil diffuse degassing at Solfatara of Pozzuoli crater, Campi Flegrei (Italy): Mapping and quantification of gas release. *J. Volcanol. Geotherm. Res.* **2014**, *289*, 26−40.
(54) Mason, R. P.; Choi, A. L.; Fitzgerald, W. F.; Hammerschmidt, C. R.; Lamborg, C. H.; Soerensen, A. L.; Sunderland, E. M. Mercury biogeochemical cycling in the ocean and policy implications. *Environ. Res.* **2012**, *119*, 101−117.
(55) Blum, J. D.; Sherman, L. S.; Johnson, M. W. Mercury isotopes in earth and environmental sciences. *Annu. Rev. Earth Planet. Sci.* **2014**, *42*, 249−269.
(56) Sun, R. Y.; Sonke, J. E.; Liu, G. J. Biogeochemical controls on mercury stable isotope compositions of world coal deposits: A review. *Earth-Sci. Rev.* **2016**, *152*, 1−13.
(57) Sun, R. Y.; Heimburger, L. E.; Sonke, J. E.; Liu, G. J.; Amouroux, D.; Berail, S. Mercury stable isotope fractionation in six utility boilers of two large coal-fired power plants. *Chem. Geol.* **2013**, *336*, 103−111.
(58) Sun, R. Y.; Sonke, J. E.; Heimburger, L. E.; Belkin, H. E.; Liu, G. J.; Shome, D.; Cukrowska, E.; Liousse, C.; Pokrovsky, O. S.; Streets, D. G. Mercury stable isotope signatures of world coal deposits and historical coal combustion emissions. *Environ. Sci. Technol.* **2014**, *48* (13), 7660−7668.
(59) Eurostat. Coal consumption statistics. http://ec.europa.eu/eurostat/statistics-explained/index.php/Coal_consumption_statistics.
(60) Donovan, P. M.; Blum, J. D.; Yee, D.; Gehrke, G. E.; Singer, M. B. An isotopic record of mercury in San Francisco Bay sediment. *Chem. Geol.* **2013**, *349-350*, 87−98.
(61) Laurier, F. J. G.; Mason, R. P.; Whalin, L.; Kato, S. Reactive gaseous mercury formation in the North Pacific Ocean's marine boundary layer: A potential role of halogen chemistry. *J. Geophys. Res.* **2003**, *108* (D17), 4529.
(62) Obrist, D.; Tas, E.; Peleg, M.; Matveev, V.; Fain, X.; Asaf, D.; Luria, M. Bromine-induced oxidation of mercury in the mid-latitude atmosphere. *Nat. Geosci.* **2011**, *4* (1), 22−26.
(63) Chevalier, A.; Gheusi, F.; Delmas, R.; Ordonez, C.; Sarrat, C.; Zbinden, R.; Thouret, V.; Athier, G.; Cousin, J. M. Influence of altitude on ozone levels and variability in the lower troposphere: a ground-based study for western Europe over the period 2001−2004. *Atmos. Chem. Phys.* **2007**, *7* (16), 4311−4326.
(64) Kohler, M. O.; Radel, G.; Shine, K. P.; Rogers, H. L.; Pyle, J. A. Latitudinal variation of the effect of aviation NOx emissions on atmospheric ozone and methane and related climate metrics. *Atmos. Environ.* **2013**, *64*, 1−9.
(65) Fitzenberger, R.; Bosch, H.; Camy-Peyret, C.; Chipperfield, M. P.; Harder, H.; Platt, U.; Sinnhuber, B. M.; Wagner, T.; Pfeilsticker, K. First profile measurements of tropospheric BrO. *Geophys. Res. Lett.* **2000**, *27* (18), 2921−2924.
(66) Seigneur, C.; Lohman, K. Effect of bromine chemistry on the atmospheric mercury cycle. *J. Geophys. Res.* **2008**, *113* (D23), D23309.
(67) Biswas, A.; Blum, J. D.; Bergquist, B. A.; Keeler, G. J.; Xie, Z. Q. Natural mercury isotope variation in coal deposits and organic soils. *Environ. Sci. Technol.* **2008**, *42* (22), 8303−8309.
(68) Hintelmann, H.; Lu, S. Y. High precision isotope ratio measurements of mercury isotopes in cinnabar ores using multi-collector inductively coupled plasma mass spectrometry. *Analyst* **2003**, *128* (6), 635−639.
(69) Sherman, L. S.; Blum, J. D.; Keeler, G. J.; Demers, J. D.; Dvonch, J. T. Investigation of local mercury deposition from a coal-fired power plant using mercury isotopes. *Environ. Sci. Technol.* **2012**, *46* (1), 382−390.


DOI: 10.1021/acs.est.6b00033
*Environ. Sci. Technol.* 2016, 50, 5641−5650

(70) Laffont, L.; Sonke, J. E.; Maurice, L.; Monrroy, S. L.; Chincheros, J.; Amouroux, D.; Behra, P. Hg Speciation and Stable Isotope Signatures in Human Hair As a Tracer for Dietary and Occupational Exposure to Mercury. *Environ. Sci. Technol.* **2011**, *45* (23), 9910−9916.
(71) Zambardi, T.; Sonke, J. E.; Toutain, J. P.; Sortino, F.; Shinohara, H. Mercury emissions and stable isotopic compositions at Vulcano Island (Italy). *Earth Planet. Sci. Lett.* **2009**, *277* (1−2), 236−243.


DOI: 10.1021/acs.est.6b00033
*Environ. Sci. Technol.* 2016, 50, 5641−5650